Egypt. J. Chem. **Vol. 68,** SI: Z. M. Nofal, pp. 417- 428 (2025)

Egyptian Journal of Chemistry

http://ejchem.journals.ekb.eg/

Removal of Arsenazo III Dye from Wastewater Using Some Nano-Engineered Ferrite and Magnetite Adsorbents

Mahmoud O. Abd El-Magied *[1], Manar Sopaih[2], Ramadan A. Abdelhafez[2], Zeinab. M. Anwar[2]

[1] *Department of Isotopes Geology, Nuclear Materials Authority, P.O. Box 530, El Maadi, 11936, Cairo, Egypt*

[2] *Chemistry Department, Faculty of Science, Suez Canal University, Egypt*

Abstract

Arsenazo III dyes are widely used in the measurement of several elements, the most important of which are uranium, thorium, and rare earth elements. Thus, the removal of arsenazo III dye, whether free or related to various water sources, is one of the important steps in preserving the environment from pollution. In this research, the possibility of removing arsenazo III from wastewater via several nanoengineered adsorbents was studied. Magnetite, zinc ferrite and magnesium ferrite were prepared, and their adsorption properties against the dye under study were studied. The study proved that the prepared materials are nanosized and have distinct adsorption properties for arsenazo III dye molecules. The uptake of Zn-ferrite, Mg-ferrite, and magnetite by arsenazo III dye is greater at pH 2.1 than at lower or higher pH values. The time-based experiments revealed that the capacity of the Zn-ferrite, Mg-ferrite, and magnetite adsorbents for arsenazo III increased over time until they reached equilibrium (20 and 100 min for the ferrite and magnetite adsorbents, respectively). The maximum capacities of the Zn-ferrite, Mg-ferrite, and magnetite adsorbents are 107.27, 113.02, and 123.46 mg/g, respectively. The results revealed that the RL values were between 0.1 and 0.5, i.e., and thus fell within the range of favorable adsorption reactions.

Keywords: Nanoengineered adsorbents; Arsenazo dye; Ferrite; Isotherm; Removal; Kinetic.

1. Introduction

Water pollution is one of the most critical environmental concerns confronting humanity today. The availability of water is the primary basis for any desired economic development and progress. Because of human activities, existing freshwater supplies are becoming increasingly contaminated and inaccessible. Chemical pollution is traditionally caused by inorganic and/or organic contaminants [1, 2]. Wastewater containing significant amounts of dyes and other organic compounds is produced in significant quantities by multiple industries [3-5]. Approximately 10,000 distinct commercial dyes are currently thought to exist, and approximately a million tons are developed globally each year [6-8]. The textile industry ranks first in dye usage, among other industries, such as rubber, paper, plastic, and cosmetics. Dyes or coloring agents are frequently utilized in various industries, such as fabrics, paper, suede or leather, and cosmetics, to add color to their products[2]. However, the release of dye-containing effluent into water bodies can have detrimental impacts on the surrounding living system, including humans [9, 10]. One such dye that is of concern is arsenazo III, a synthetic dye commonly used in many industries, including the textile and paper industries [11]. Additionally, arsenazo III is a common spectrophotometric indicator in different analytical fields for the sensing and quantification of various metal ions. Arsenazo III is widely used in the determination of metal ions, particularly in the spectrophotometric determination of a variety of metal ions, such as uranium, rare earth elements, arsenic, cadmium, zinc, and nickel. Arsenazo III is a water-soluble dye that can endanger aquatic life and disrupt the natural balance of ecosystems. Despite its usefulness in analytical chemistry, arsenazo III poses environmental hazards because of its toxic nature. Exposure to arsenazo III can cause skin irritation, eye damage, and respiratory problems. Arsenazo III is classified as a hazardous substance by various regulatory bodies because of its potential toxicity and carcinogenicity. Therefore, it is essential to manage arsenazo III with caution and dispose of it properly to prevent environmental contamination. Therefore, removing arsenazo III from water bodies is essential for reducing its impact on living systems and human health[12].

*Corresponding author e-mail: mahmoud_nma@yahoo.com.; (**Mahmoud O. Abd El-Magied**).

Received date 08 April 2025; Revised date 11 May 2025; Accepted date 03 June 2025

DOI: 10.21608/EJCHEM.2025.373841.11563

A range of methods are available to remove arsenazo III from its effluent, including physical, chemical, and biobased methods (coagulation, biological precipitation and adsorption methods) [9, 10, 13, 14]. In coagulation and precipitation methods, a coagulant or a precipitating agent is added to wastewater to form insoluble complexes with arsenazo III dye molecules, which can then be easily separated from the water. Biological methods are approaches for removing arsenazo III from its effluent. In biological methods, microorganisms are used to break down arsenazo III species into harmless byproducts. Certain bacteria and fungi can metabolize and break down dye molecules, converting them into nontoxic compounds. However, the benefits of biological treatment may vary according to the specific properties of the Arsenazo III species, and the microbial strains used. Owing to low dye biodegradation, a conventional biological treatment process is not highly profitable for wastewater disposal [15]. Another effective method for the removal of arsenazo III from wastewater is adsorption, where arsenazo III dye molecules are attracted to a solid surface and trapped, effectively removing them from wastewater [11, 12, 16, 17]. Adsorption approaches have many advantages and therefore many applications compared with other pollutant removal processes [18-23].

There is interest in innovative technologies developed to remove organic dyes from their effluent and reduce their hazardous impact on organisms and humans [24]. Among the more interesting techniques for achieving this goal is the use of nanoengineered adsorbents. Nanoengineered adsorbents offer high reactivity owing to their nanosized dimensions. These characteristics increase their absorptivity, making them effective at capturing and removing arsenazo III dyes from water. Nanoparticles (NPs) have gained significant interest because of their unusual characteristics (physicochemical properties), along with their wide-ranging potential applications in the environmental, medical, tissue engineering, analytical, and petroleum industries. In this context, the elimination of arsenazo III species from wastewater utilizing some synthesized adsorbents will be a matter of concern during this study (to eliminate their chemical toxicity).

2. Experimental

3.1. Chemicals and Apparatus

The chemicals used were high-purity chemicals produced by Sigma–Aldrich, and all of them were used without further purification steps. Distilled water was used to make all the solutions, which was also used to wash the prepared products. The pH of the medium was adjusted via the use of diluted solutions of HCl and NaOH. Ferric chloride, ferrous chloride, magnesium chloride and zinc chloride were used to generate their respective ions.

3.2. Synthesis of nanoengineered adsorbents

The nanoengineered adsorbents, magnesium and zinc ferrite nanoparticles, were synthesized via the combustion method [25-27], where magnetite nanoparticles were prepared via the coprecipitation method [28, 29]. For magnesium and zinc ferrite nanoparticles, the stoichiometric concentrations of magnesium, iron and zinc chloride salts were dissolved in separate aqueous solutions. The previous three solutions were stirred until completely dissolved (clear solutions were obtained). In two separate reactors, iron and magnesium solutions were mixed, and iron and zinc solutions were combined and agitated for approximately one hour. The acetic acid solution served as a precursor in the reaction. Acetic acid is five times more concentrated than the metal ions utilized. The acetic acid was dissolved and combined with the solutions in the previous two reactors and stirred for 120 min. The pH of the medium was adjusted to that of the base medium. The grade of the previous reactors was increased to 85 °C to allow self-combustion of the prepared products. The products obtained were rinsed to eliminate contaminants, and subsequently, the products were dried at a relatively high level (650 °C) to eliminate acetic acid (precursor) and obtain nanoengineered adsorbents (magnesium ferrite (Mg-ferrite) and zinc ferrite nanoparticles (Zn-ferrite)) [27]. The magnetite adsorbent was prepared by pairing iron(II) and iron(III) ions in their solutions. In detail, separate solutions of iron(II) and iron(III) ions were made by dissolving their salts in oxygen-free water, where the resulting solutions were mixed directly with each other and stirred very quickly. The ammonia solution was put in the prior solution to precipitate the iron(II) and iron(III) ions together, and this step was performed with extreme stirring until a black precipitate formed. The mixture was stirred for 40 minutes to allow the formed magnetite (iron(II) and iron(III) hydroxides) to crystallize. The magnetite formed in the solution was separated via a centrifuge and carefully rinsed with distilled water to eliminate contaminants. The magnetite formed was washed until the acidity of the washing solution medium was neutral. After that, the product was dried at 105 °C. The nanoengineered adsorbents, magnesium ferrite, zinc ferrite, and magnetite nanoparticles, were characterized via DLS, FT-IR, XRD, SEM, and EDX analysis.

3.3. Adsorption measurements via the batch method

In adsorption experiments, the batch technique is commonly used to evaluate the adsorption properties of various materials. This technique involves an adsorbent (solid phase) in a solution containing the molecules to be adsorbed (adsorbate, liquid phase). By monitoring the initial concentration (before shaking) and equilibrium concentration (after shaking) of molecules to be adsorbed in the system, the amount of molecules adsorbed onto the sorbent surface can be determined. Therefore, the numerous factors that affect this process should be studied and addressed. Arsenazo III elimination from wastewater is important for creating an effective and sustainable treatment process. The studied factors include pH, time, and the quantity of Zn-ferrite, Mg-ferrite, magnetite, and arsenazo III. The experiments were performed via the batch technique. The role of acidity in the adsorption process was determined by combining the adsorbent nanoparticles (0.01g) with arsenazo III solution (0.02) at various pH values (1.04-9.0) in a flask and shaking the mixture for a certain period. To investigate the influence of duration on the uptake process, the adsorbent nanoparticles (0.01g) were shaken in the arsenazo III solution (0.02 L) at different time intervals (5-180 min). The outputs from the prior experiments were used to determine the system's kinetics. One crucial factor that can influence the uptake of arsenazo III is its initial content in the effluents being treated. The impact of the

initial arsenazo III concentration on the adsorption process was assessed by agitating the adsorbent nanoparticles (0.01g) shaken in the arsenazo III solution (0.02 L) of different initial concentrations (8-120 mg/L). To study the effects of the solid/liquid ratio on the process, adsorption experiments were conducted, with the Zn-ferrite, Mg-ferrite, and magnetite adsorbents being shaken in a solution containing a known adsorbate concentration. The solid/liquid ratio was varied by varying the content of adsorbent (0.005-0.105 g) while keeping the solution volume constant (0.02 L, 100 mg/L). After shaking the arsenazo III/adsorbent solution for a set period, the remaining arsenazo III species were measured.

3. Results and discussion

2.1. Characterization

The adsorbent materials were analyzed via FT-IR to identify the functional groups contained in the zinc ferrite (Zn-ferrite), magnesium ferrite (Mg-ferrite), and magnetite materials. Fig.1 shows the results of the FT-IR analysis of the prepared nanomaterials. Fig. 1 shows the appearance of the element-oxygen bond (Mg, Fe, and Zn) at the wavenumbers (cm^{-1}) of 1513-1653 cm^{-1} and 447-697 cm^{-1} [25, 26]. The synthesis of magnetite was confirmed by FT-IR, as shown in Fig. 1. The spectrum confirms the existence of Fe–O stretching (bands at 580, 650 and 750 cm^{-1}).

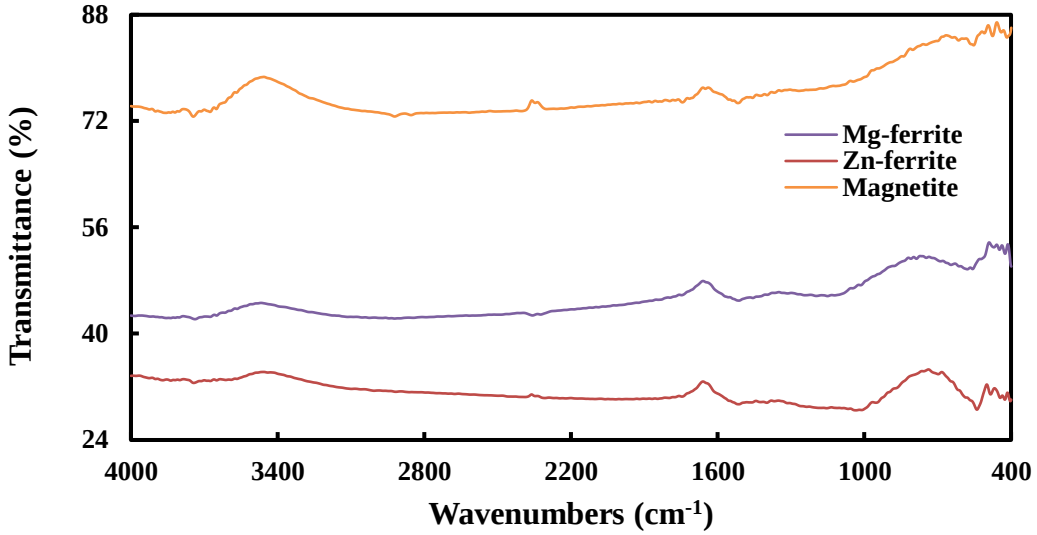

Fig. 1 FT-IR spectra of free Zn-ferrite, Mg-ferrite, and magnetite

Nanomagnetite was prepared and characterized according to our previously published methods [28]. For other nanoparticles, analyses have shown success in their preparation. Scanning electron microscopy (SEM) is a powerful imaging technique that provides high-resolution images of the surface morphology of materials. SEM-based assessment, combined with EDX, offers a comprehensive analysis of the morphology, particle size, and elemental composition of Zn-ferrite and Mg-ferrite. Fig. 2 shows the SEM images and shapes of the material surfaces. Energy dispersive X-ray spectroscopy (EDX) is a powerful analytical technique used to determine the elemental composition of materials. EDX-based assessment provides a detailed and quantitative analysis of the elemental composition of Zn-ferrite and Mg-ferrite. Also, the EDX-based assessment of the Zn-ferrite and Mg-ferrite compositions demonstrated that magnetite consists of iron and oxygen; that zinc ferrite consists of zinc, iron and oxygen; and that magnesium ferrite consists of magnesium, iron and oxygen, which confirms the precision of the preparation of Zn-ferrite, Mg-ferrite, and magnetite components. The presence and intensity of the Zn and Mg peaks into the EDX charts of Zn-ferrite and Mg-ferrite confirm the incorporation of these elements into the ferrite structure.

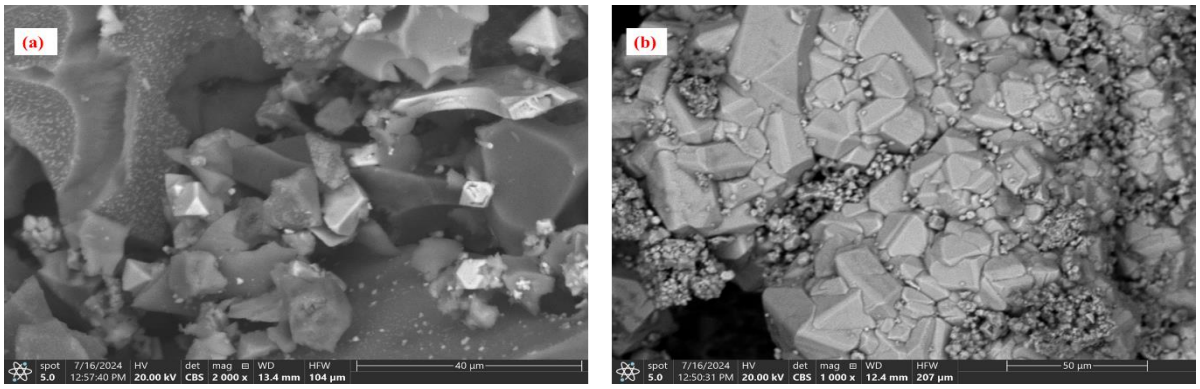

Fig. 2 SEM images of Zn-ferrite (a) and Mg-ferrite (b).

2.2. Adsorption parameters

Multiple factors (pH, time, and the S/L ratio) affect the removal of arsenazo III from wastewater via solid adsorbents. Each of these factors is critical in determining the effectiveness of the removal process. Therefore, understanding and optimizing these factors are crucial for maximizing efficient arsenazo III removal from solutions.

The adsorption capacity (q_e, mg of adsorbate per g of adsorbent) and efficiency (q_e (%), amount of arsenazo III species adsorbed onto the Zn-ferrite, Mg-ferrite, and magnetite surfaces relative to the whole amount of arsenazo III species) were determined via Equations 1 and 2 [30, 31].

$$q_e \left(\frac{mg}{g}\right) = \frac{C_i - C_e}{ads.\,wt.} \times V \qquad (1)$$

$$q_e\,(\%) = \frac{(C_i - C_e) \times 100}{C_i} \qquad (2)$$

where ads.wt. and V are the weights of adsorbent (g) and the volume of arsenazo III solution (L), respectively. C_i and C_e are the initial and equilibrium arsenazo III species concentrations (mg/L), respectively.

2.2.1. Effect of pH on arsenazo III removal

The acidity of the adsorption system is a key factor influencing arsenazo III adsorption [16, 32]. The pH can have a major effect on the electrostatic properties of both adsorbate species and the adsorbent surface . Understanding how pH affects arsenazo III adsorption by Zn-ferrite, Mg-ferrite, and magnetite is essential for optimizing wastewater treatment system design and increasing the effectiveness of arsenazo III removal.

To understand how pH affects arsenazo III adsorption by Zn-ferrite, Mg-ferrite, and magnetite, experiments were conducted by stirring their particles in an arsenazo III solution (with different pH values). These findings indicate that pH has a substantial role in arsenazo III removal by the adsorbents used, Fig. 3(a). The uptake of arsenazo III dye by Zn-ferrite, Mg-ferrite, and magnetite is greater at pH 2.1 than at lower or higher pH values. The effect of pH may result from its influence on the electrical charge on the surface of the Zn-ferrite, Mg-ferrite, magnetite and arsenazo III species, which in turn affects the entire adsorption process.

The higher capacity of Zn-ferrite, Mg-ferrite, and magnetite for arsenazo III at pH 2.1 may be explained by the electrostatic binding between arsenazo III molecules (negatively charged) and Zn-ferrite, Mg-ferrite, and magnetite surfaces (positively charged due to protonation effects). As the pH increased, the content of hydroxyl groups that compete for binding sites with anionic Arsenazo III dyes increased, resulting in a decreasing in the adsorption capability. Additionally, the surfaces of Zn-ferrite, Mg-ferrite, and magnetite and the anionic dye arsenazo III are negatively charged at relatively high pH; consequently, the repulsion force between the two terms causes the adsorption capacity to decrease [11].

2.2.2. Effect of initial arsenazo III concentration

The initial concentration of the arsenazo III species in wastewater influences its removal efficiency. As a result, determining the optimal arsenazo III concentration in wastewater is critical for achieving maximum removal efficiency. To measure the influence of starting arsenazo III species on the process, various arsenazo III concentrations (8 to 120 mg/L) were treated with Zn-ferrite, Mg-ferrite, and magnetite absorbents. The relationship between the arsenazo III concentration and adsorption efficiency may be evaluated by comparing the quantity of adsorbed arsenazo III species at various initial concentrations, Fig. 3(b). The results of these experiments demonstrated that increasing the arsenazo III concentration enhances the adsorption ability (because more dye molecules are available for adsorption). However, this capacity becomes constant after the initial concentration of dye is reached (as the active sites become saturated with dye molecules).

Therefore, lower initial concentrations of dye result in lower amounts of dye being adsorbed onto the Zn-ferrite, Mg-ferrite, and magnetite adsorbents (lower adsorption capacities), as fewer dye molecules may be adsorbed. This can result in lower adsorption capacities and slower adsorption rates. However, in contrast, higher initial concentrations of dye result in more arsenazo III adsorbed onto the Zn-ferrite, Mg-ferrite, and magnetite adsorbents. This is because at higher concentrations, more dye molecules may be adsorbed, which enhances the adsorption capability . At the optimum initial concentration, the maximum number of arsenazo III species that can be adsorbed by the adsorbents is reached, and any further increase in the arsenazo III concentration will not result in increased adsorption capacity [33]. Therefore, the capacity of Zn-ferrite, Mg-ferrite, and magnetite adsorbents become constant after the optimum initial concentration of dye (100 mg/L) is reached.

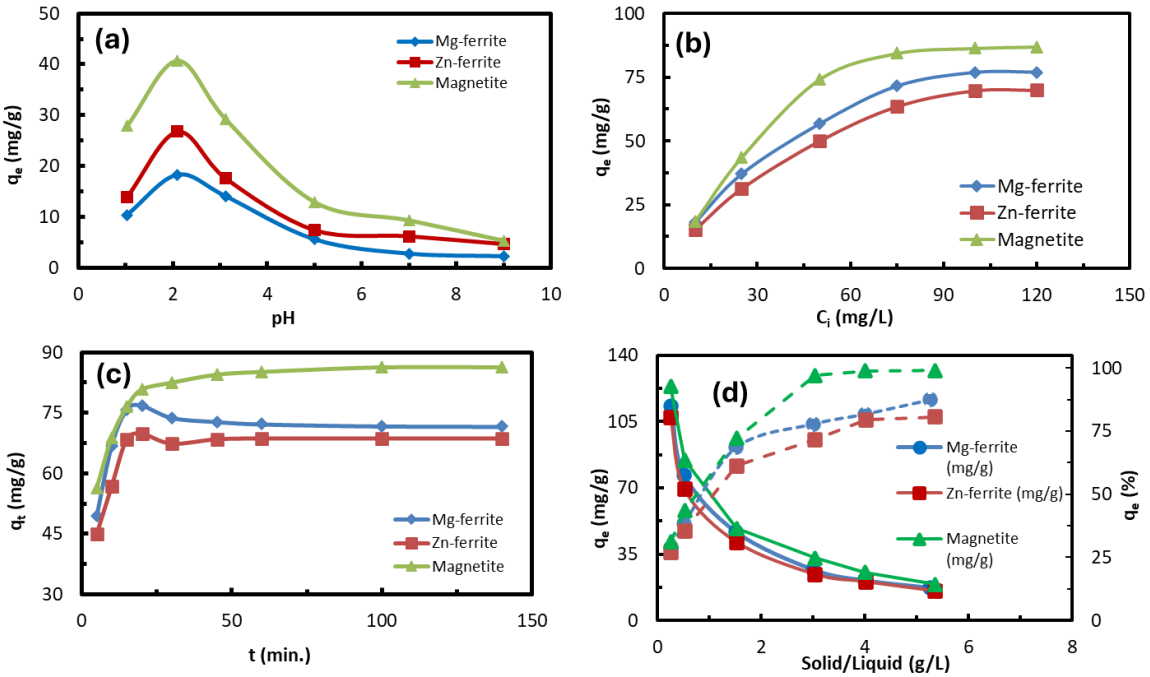

Fig. 3 Effects of pH (a), arsenazo III concentration (b), time (c), and solid/liquid ratio (d) on arsenazo III adsorption by Zn-ferrite, Mg-ferrite, and magnetite adsorbents.

2.2.3. Effect of time

Contact time is another crucial factor that influences arsenazo III removal (capacity and efficiency) from wastewater by solid adsorbents. The time-based experiments revealed that the capacity of Zn-ferrite, Mg-ferrite, and magnetite adsorbents for arsenazo III increased as time progressed until reaching equilibrium (20 and 100 min for the ferrite and magnetite adsorbents), where the rate of arsenazo III adsorption was equal to the rate of arsenazo III desorption. This occurred because as the arsenazo III species encounter adsorbent particles for a longer period, more dye molecules can bind to the Zn-ferrite, Mg-ferrite, and magnetite surfaces. However, after the optimum time, the capacity of Zn-ferrite, Mg-ferrite, and magnetite for arsenazo III becomes constant. At the optimum time, the maximum amount of arsenazo III species that may bind the surface of Zn-ferrite, Mg-ferrite, and magnetite has been reached (the adsorbent surfaces are saturated with dye molecules). Any additional time spent on treating solutions with the adsorbent particles will not result in further adsorption, Fig. 3(c).

2.2.4. Effect of solid/liquid ratio

The solid/liquid ratio, or the ratio of the solid phase (adsorbent) to the volume of the liquid phase (volume of solution), is a key parameter that might affect the adsorption process [34]. Adsorption tests were conducted in which the Zn-ferrite, Mg-ferrite, and magnetite adsorbents were shaken in a solution containing a known arsenazo III concentration to determine the effects of the solid/liquid ratio, Fig. 3(d). The solid/liquid ratio varied by varying the amount of Zn-ferrite, Mg-ferrite, and magnetite adsorbents (from 0.05 to 0.105 g), and the volume of arsenazo III was constant (0.02 liters). These findings demonstrated that while the adsorption efficiency increased with increasing solid/liquid ratio, the adsorption capacity decreased. The number of dye species that may bind the adsorbent's surface in relation to the total amount of dye species (the initial amount of dye species) determines the adsorption efficiency of the Zn-ferrite, Mg-ferrite, and magnetite adsorbents. The relatively high removal efficiency might have resulted from the increased Zn-ferrite, Mg-ferrite, and magnetite adsorbents increasing the surface area accessible for arsenazo III adsorption. A greater amount of adsorbent provides more surface area for the arsenazo III adsorbate, leading to greater binding of arsenazo III onto the surface of the Zn-ferrite, Mg-ferrite, and magnetite adsorbents. Additionally, a higher solid/liquid ratio can also lead to more collisions between the arsenazo III molecules and the Zn-ferrite, Mg-ferrite, and magnetite adsorbents (enhanced adsorption). Additionally, the weight of the arsenazo III species that may be adsorbed per weight of adsorbent (mg of adsorbate per g of adsorbent) of the Zn-ferrite, Mg-ferrite, and magnetite adsorbents decreases as the dosage increases. The surfaces of the Zn-ferrite, Mg-ferrite, and magnetite adsorbents become saturated with dye molecules at higher adsorbent doses, which lowers the capacity. The maximum efficiencies (q_e, %) of the Zn-ferrite, Mg-ferrite, and magnetite adsorbents are 87.35, 84.00, and 98.93%, respectively. On the other hand, the maximum capacities (q_e, mg/g) of the Zn-ferrite, Mg-ferrite, and magnetite adsorbents are 107.27, 113.02, and 123.46 mg/g, respectively.

2.3. Adsorption isotherms

Adsorption isotherms play a basic role in understanding the adsorptive behavior of different systems and optimizing adsorption processes. Adsorption isotherms elucidate the interactions between adsorbate molecules and adsorbent surfaces.

Evaluations of isotherms are crucial for characterizing the adsorptive properties of various materials and comparing their performance. Studying the adsorption isotherm of a particular adsorbent material may determine its suitability, assess its capacity, and compare it with those of other materials [35]. The isotherm data also allows for the calculation of important parameters. The Langmuir isotherm is a more widely used model to describe adsorption processes [16, 36, 37]. The Langmuir model assumes that adsorption occurs on a homogeneous surface and that adsorbate molecules do not interact with each other once adsorbed. The model also assumes that fixed binding sites are involved in adsorption and that adsorption is a reversible process .The Langmuir model is important in adsorption processes for several reasons. It provides an easy and effective tool for analyzing experimental data and determining key parameters such as the maximum theoretical capacity and equilibrium binding constant. Equation 3 presents the Langmuir model in its linear form [38, 39].

$$\frac{C_e}{q_e} = \frac{C_e}{Q_{max}} + \frac{1}{K_L Q_{max}} \qquad (3)$$

where K_L and Q_{max} are constants called the Langmuir binding constant and the maximum theoretical capacity (theoretical capacity), respectively. The experimental data was processed via Equation 3 to analyze the susceptibility of the Langmuir model to describe the effects of arsenazo III removal on Zn-ferrite, Mg-ferrite, and magnetite adsorbents. The plots of C_e/q_e with C_e are drawn on Fig. 4 (a). The model plots are straight lines indicating their suitability for describing arsenazo III removal by Zn-ferrite, Mg-ferrite, and magnetite adsorbents (Table 1). The high straightness of the lines (R^2) proves its suitability for interpreting the removal of arsenazo III dye from its sources via Zn-ferrite, Mg-ferrite, and magnetite adsorbents. The results also show that the theoretical adsorption capacity values (Q_{max}) are approximately equal to the practical values from the experiments, which confirms the ability of the model to explain the removal of arsenazo III from its solutions via Zn-ferrite, Mg-ferrite, and magnetite adsorbents. One important parameter that characterizes the Langmuir model is the separation factor or equilibrium parameter (R_L). This parameter is defined as $R_L = 1/(1 + K_L C_i)$, where K_L is the Langmuir constant. The equilibrium parameter (R_L) helps in understanding and analyzing adsorption processes. It provides valuable information and helps in determining the validity and feasibility of whole processes. The separation factor is a measure of the favorability of adsorption, with $R_L < 1$ indicating favorable adsorption, $R_L = 1$ indicating linear adsorption, and $R_L > 1$ indicating unfavorable adsorption. The results revealed that the equilibrium parameter (R_L) values approximately fall between 0.1 and 0.5, i.e., and thus fall within the range of favorable adsorption reactions, Fig. 4(b). The Langmuir approach involves adsorption occurring only at specific binding sites on the adsorbent surface, and once a molecule is adsorbed at a site, no other molecule can occupy that site. As a result, the monolayer of arsenazo III species is formed on the Zn-ferrite, Mg-ferrite, and magnetite surfaces. Therefore, these approaches are useful for describing the monolayer coverage (single-layer coverage or θ) of arsenazo III species on Zn-ferrite, Mg-ferrite, and magnetite surfaces. The surface coverage equals the fraction of Zn-ferrite, Mg-ferrite, and magnetite surfaces covered by arsenazo III species at equilibrium, Equation 4. It is a measure of the extent to which the surface is occupied by adsorbate molecules [40].

$$\theta = \frac{K_L C_i}{1 + K_L C_i} \qquad (4)$$

The single-layer coverage values of the absorbent materials are high and close to 1 (a value of 1 means that the surface is fully filled with dyes). These values confirm the high efficiency of the Zn-ferrite, Mg-ferrite, and magnetite in dye absorption.

Table 1 Outcomes of the Langmuir parameters

Adsorbent	q_e (mg/g)	Q_{max} (mg/g)	K_L (L/mg)	R^2
Mg-ferrite	76.98	83.33	0.1476	0.9946
Zn-ferrite	69.98	76.34	0.1331	0.9972
Magnetite	86.96	90.91	0.3235	0.9999

The Freundlich model is frequently used to predict adsorption behavior and is an important model in adsorption processes [41]. The model assumes that the sorption process is a multilayer phenomenon where the adsorbate species binds a nonuniform distribution surface (heterogeneous) with many active site types accessible for adsorption. The model can be described by Equation 5 [42].

$$\log q_e = \frac{\log C_e}{n} + \log K_F \qquad (5)$$

where K_F and n are the Freundlich binding constant and theoretical capacity (mg/g), respectively. The results of the arsenazo III removal experiments using Zn-ferrite, Mg-ferrite, and magnetite were analyzed via Equation 5 to analyze the susceptibility of the Freundlich equation to removing the dyes on the adsorbents. The relationship between the values of log (q_e) and log (C_e) is shown in Fig. 4(c). The K_F values of the model differ significantly from the experimental values from the adsorption experiments, indicating the inappropriateness of using the Freundlich model to fit arsenazo III removal via Zn-ferrite, Mg-ferrite, and magnetite (Table 2). Additionally, the resulting Freundlich line straightness is lower than the straightness of the lines produced by the Langmuir line. Therefore, the R^2 values of the Freundlich model are lower than those of the Langmuir model, confirming that the current extraction process follows the Langmuir isotherm or the single-layer adsorption model.

Table 2 Outcomes of the Freundlich parameters

Adsorbent	q_e (mg/g)	K_F (mg/g)	1/n	R^2
Mg-ferrite	76.98	19.17	0.3385	0.9879
Zn-ferrite	69.98	16.36	0.3510	0.9793
Magnetite	86.96	24.75	0.3313	0.9013

One of the important models used to describe adsorption processes is the Dubinin–Radushkevich model [43]. The Dubinin–Radushkevich model, Equation 6, was used to analyze the removal of dyes by the adsorbents [44].

$$\ln q_e = \ln Q_{DR} - K_{DR}(\varepsilon)^2 \quad \text{where } \varepsilon = RT \ln\left[1 + \frac{1}{C_e}\right] \qquad (6)$$

where Q_{DR} and ε are the theoretical capacity (mg/g) and Dubinin–Radushkevich (Polanyi potential constant related gas constant (R, 8.314 J/mol K), temperature (T, K), and equilibrium adsorbate concentration (C_e, mg/L), respectively. The plots of the ln (q_e) value against the squared values of the Polanyi potential (ε) are drawn in Fig. 4(d). The Dubinin–Radushkevich isotherm gives straight lines with high R^2 values, indicating that the Dubinin–Radushkevich isotherm may fit arsenazo III removal via Zn-ferrite, Mg-ferrite, and magnetite adsorbents (Table 3). Additionally, the theoretical adsorption capacity (Q_{DR}, mg/g) was fitted with the experimental value (q_e, mg/g), which confirms the ability of the Dubinin–Radushkevich isotherm to explain the current adsorption process. The Dubinin–Radushkevich model provides several outcomes that are valuable for understanding adsorption processes. The model allows for the determination of the Dubinin–Radushkevich constant (E). The mean adsorption energy (E) is a key parameter in the Dubinin–Radushkevich model and may be determined via Equation 7 [27].

$$E = \left[\frac{1}{\sqrt{2K_{DR}}}\right] \qquad (7)$$

The E values for arsenazo III removal via the adsorbents were found to be between 8451.54 and 9128.71 J/mol (Table 3). The calculated E values are within the range of adsorption chemical reactions.

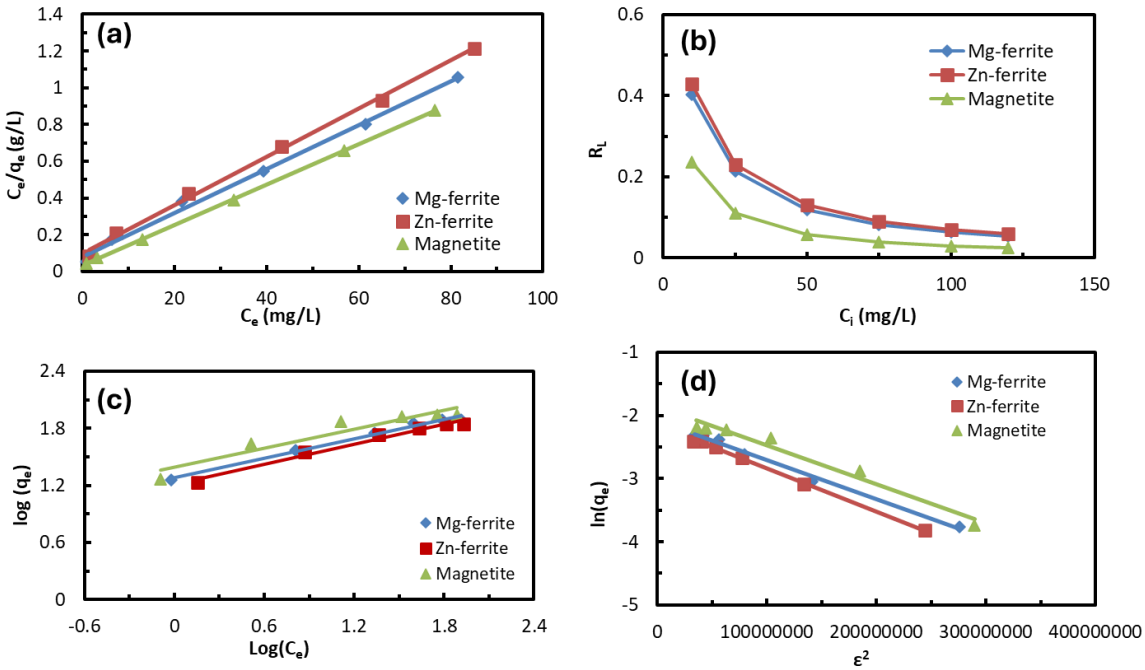

Fig. 4 Langmuir isotherm plots (a), separation factor (b), Freundlich isotherm (c), and Dubinin–Radushkevich isotherm plots (d) for arsenazo III removal by Zn-ferrite, Mg-ferrite, and magnetite adsorbents

Table 3 Outcomes of the Dubinin–Radushkevich isotherm

Adsorbent	q_e (mg/g)	Q_{DR} (mmol/g)	Q_{DR} (mg/g)	K_{DR} (mol^2/kJ^2)	E (J/mol)	R^2
Mg-ferrite	76.98	0.1237	96.06	6×10^{-9}	9128.71	0.9918
Zn-ferrite	69.98	0.1161	90.13	7×10^{-9}	8451.54	0.9985
Magnetite	86.96	0.1659	128.82	6×10^{-9}	9128.71	0.9741

2.4. Kinetic studies

The kinetics of arsenazo III removal via the studied adsorbents are crucial for determining the efficiency of Zn-ferrite, Mg-ferrite, and magnetite adsorbents in removing contaminants from wastewater. Understanding the kinetic parameters helps in designing treatment systems and predicting the activity and efficiency of adsorbents in removing contaminants [10]. To study and predict the kinetic parameters, various models have been developed. One of the commonly used models is the pseudo-first-order model. The pseudo-first-order model posits that the process is governed by the rate at which adsorbate species approach and adhere to the adsorbent surface[10]. Mathematically, the pseudo-first-order model is represented by Equation 8 [45].

$$\log (q_e - q_t) = \log(Q_1) - \frac{k_1}{2.303} t \quad (8)$$

where q_t, Q_1, and k_1 are the amount of arsenazo III adsorbed at time t (mg/g), the theoretical amount of arsenazo III adsorbed (mg/g), and the rate constant of pseudo-first-order adsorption (1/min), respectively. The values of the q_t, Q_1, and k_1 constants were determined by processing the adsorption data via Equation 8. An illustration of the link between log (q_e -q_t) and t is provided on Fig. 5(a). The results did not follow a very straight line, reflecting the inability to use the model to interpret experimental data obtained from previous experiments.

Table 4 Outcomes of the pseudo-first-order model

Adsorbent	q_e(mg/g)	Q_1(mg/g)	k_1(min^{-1})	R^2
Mg-ferrite	76.98	175.27	0.3284	0.9531
Zn-ferrite	69.98	135.61	0.2874	0.9095
Magnetite	86.96	26.58	0.0576	0.9377

The pseudo-second-order model is one of the prevalent kinetic models for adsorption processes and states that the sorption rate is precisely proportional to the square of the amount of adsorbate on the adsorbent surface [10]. The pseudo-second-order model is often preferred over other kinetic models because of its simplicity and accuracy in describing the sorption process. Equation 9 is used to represent the pseudo-second-order model. The possibility of pseudo-second-order kinetics can be validated through experimental data via linear plots of t/qt versus time to determine the rate constants and evaluate the adsorption mechanism, thus providing valuable insights for applications in environmental remediation.

$$\frac{t}{q_t} = \frac{1}{k_2 Q_2^2} + \frac{1}{Q_2} t \quad (9)$$

where k_2 is the rate constant of the pseudo-second-order model and where Q_2 is the adsorption capacity of the model. The plots obtained are straight lines, and the reactions may follow pseudo-second-order kinetics. The values of k_1 and q_1 were predicted by fitting the experimental data to the pseudo-second-order model (Fig. 5(b)). The findings also show that the theoretical adsorption capacity values of the model are roughly the same as or comparable to the actual values from the adsorption experiments (Table 5). The findings demonstrated that the rule produced a straight line, suggesting that the adsorption process could be explained by the model.

Table 5 Outcomes of the pseudo second-order model

Adsorbent	q_e(mg/g)	Q_2(mg/g)	k_2(g/mg.min)	R^2
Mg-ferrite	76.98	95.24	0.0023	0.9957
Zn-ferrite	69.98	87.72	0.0023	0.9937
Magnetite	86.96	88.50	0.0046	0.9999

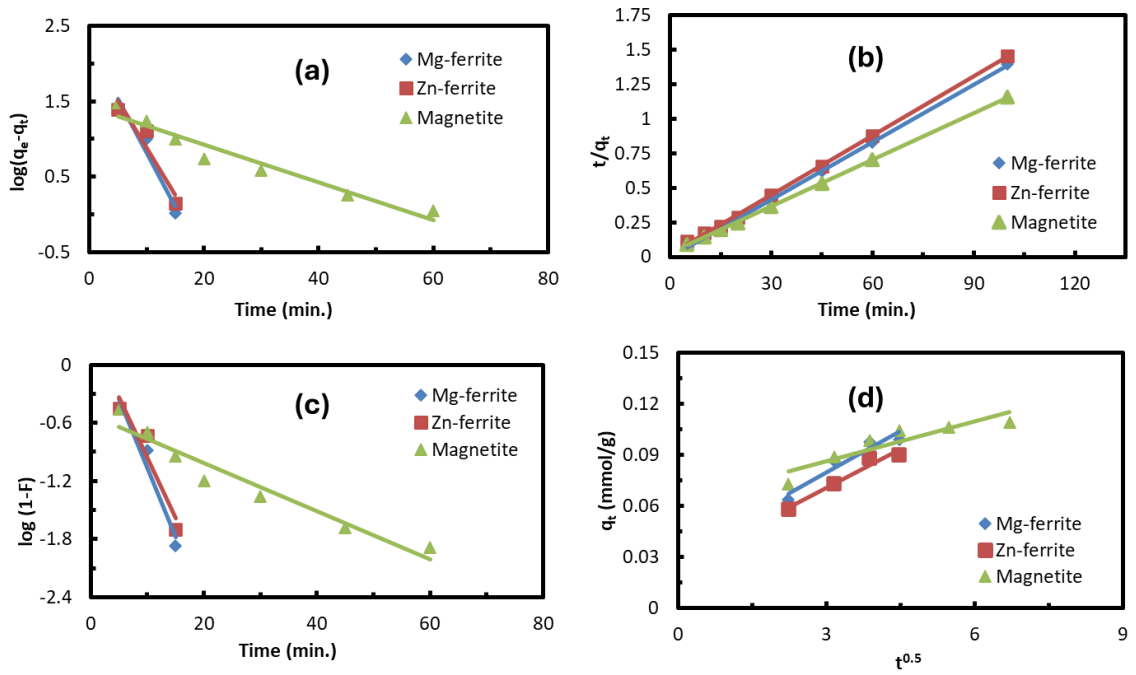

Fig. 5 (a) Pseudo-first order (a), pseudo-second-(b), liquid film diffusion (c), and intraparticle diffusion (d) models for arsenazo III removal via Zn-ferrite, Mg-ferrite, and magnetite adsorbents

Adsorption is a surface process where molecules adhere to a solid [16]. It involves stages such as bulk diffusion, thin film diffusion, intraparticle diffusion, and adsorption interactions. In stirred systems, bulk diffusion is less significant due to reduced mass transfer resistance, whereas liquid film diffusion can notably impact adsorption by affecting how adsorbate molecules move through the surrounding liquid film. The liquid film diffusion model suggests that adsorption occurs at the solid–liquid interface, where adsorbate molecules diffuse through a liquid film to the solid surface. Mass transfer is limited by this diffusion, which is determined by the film thickness and the concentration gradient. The film thickness also varies with temperature and concentration. Understanding these models is crucial for understanding mass transfer in adsorption and the influence of liquid film mechanisms. This model can be expressed with Equation [33].

$$\log(1 - F) = -\frac{k_{LF}}{2.303} t \qquad (10)$$

F, k_{LF}, and t are constant (F denotes the ratio of q_t/q_e), rate constant and time. When analyzing the data, if the plot of log(1-F) against (t) produces a straight line, characterized by a high coefficient (R^2) and a zero intercept, this observation strongly suggests that the flow of dyes species through the liquid film is the rate-determining step in the overall adsorption process. Fig. 5(c) and Table 6 highlight the significance of the liquid film's dynamics in controlling the rate of adsorbate uptake.

Table 6 Outcomes of the liquid film diffusion model

Adsorbent	Intercept	k_{LF} (min^{-1})	R^2
Mg-ferrite	0.3579	0.3284	0.9531
Zn-ferrite	0.2887	0.2874	0.9095
Magnetite	-0.5118	0.0576	0.9377

The intraparticle diffusion of arsenazo III within Zn-ferrite, Mg-ferrite, and magnetite pores (the third step in the adsorption process) plays an important role in the adsorption of dyes on porous solid adsorbents. This step represents the transport of adsorbate molecules from the bulk solution to the solid surface through the pores of Zn-ferrite, Mg-ferrite, and magnetite [10]. According to the intraparticle diffusion hypothesis, the rate-limiting step in adsorption processes is the transport of arsenazo III molecules from the bulk solution to the solid surface through the pores of the Zn-ferrite, Mg-ferrite, and magnetite adsorbents [10]. This model is represented by the following equation (Equation 11) [33]:

$$q_t = k_{IPD} t^{1/2} + C \qquad (11)$$

The former equation of the model yields the initial adsorption rate constant (k_{IPD}) and the boundary layer effect constant (C). The plot of q_t versus ($t^{0.5}$) produced straight lines, as shown in Fig. 5(d). Table 7 indicates that the rate-determining step of arsenazo III removal via Zn-ferrite, Mg-ferrite, and magnetite adsorbents is influenced by the transport of arsenazo III molecules from the bulk solution to the solid surface through the pores of the Zn-ferrite, Mg-ferrite, and magnetite adsorbents.

Table 7: Outcomes of the intraparticle diffusion model

Adsorbent	C	K_{IPD} (mg/g $min^{0.5}$)	R^2
Mg-ferrite	0.0304	0.0163	0.9212
Zn-ferrite	0.0252	0.0151	0.9573
Magnetite	0.0613	0.077	0.8178

5. Conclusions

Removing arsenazo III from water is crucial for mitigating environmental and health risks associated with dye pollution. This study investigated the efficacy of nanoengineered magnesium ferrite, zinc ferrite, and magnetite nanoparticles as adsorbents for arsenazo III removal from wastewater. These adsorbents, synthesized via combustion and coprecipitation methods, were tested in batch experiments, examining the influence of pH, contact time, adsorbent dosage, and arsenazo III concentration. Results indicated that pH significantly impacts removal efficiency, with lower pH values (specifically pH 2.1) promoting greater adsorption due to increased positive surface charge on the adsorbents. While adsorption efficiency increased with higher solid/liquid ratios, adsorption capacity decreased. Maximum removal efficiencies were 87.35%, 84.00%, and 98.93% for zinc ferrite, magnesium ferrite, and magnetite, respectively. Langmuir and Dubinin-Radushkevich isotherm models effectively described the adsorption process, with theoretical adsorption capacity values closely matching experimental results. High single-layer coverage values near 1 confirm the materials' effective dye absorption. Dubinin-Radushkevich isotherm fitting showed good linear fits. Furthermore, energy values (E) between 8.45 and 9.13 kJ/mol suggest a chemical adsorption mechanism. Pseudo-second-order kinetics adequately described the adsorption process, with intraparticle diffusion influencing the rate-determining step of arsenazo III removal.

Declarations

Funding

No funds, grants, or other support was received.

Competing interests

The authors have no relevant financial or nonfinancial interests to disclose.

References

[1] M. Tabish, A.B. Tabinda, Z. Mazhar, A. Yasar, J. Ansar, I. Wasif, Physical, chemical and biological treatment of textile wastewater for removal of dyes and heavy metals, Desalination and Water Treatment, 320 (2024) 100842. DOI: 10.1016/j.dwt.2024.100842

[2] A.P. Periyasamy, Recent advances in the remediation of textile-dye-containing wastewater: Prioritizing human health and sustainable wastewater treatment, Sustainability, 16 (2024) 495. DOI: 10.3390/su16020495

[3] N. Loura, K. Rathee, R. Dhull, M. Singh, V. Dhull, Carbon nanotubes for dye removal: A comprehensive study of batch and fixed-bed adsorption, toxicity, and functionalization approaches, Journal of Water Process Engineering, 67 (2024) 106193. DOI: 10.1016/j.jwpe.2024.106193

[4] J. Lagiewka, K. Witt, M. Gierszewska, I. Zawierucha, Selective removal of organic dyes via polymer inclusion membrane containing a perbenzylated β-cyclodextrin derivative, Journal of Water Process Engineering, 68 (2024) 106306. DOI: 10.1016/j.jwpe.2024.106306

[5] C. Miao, W. Huang, K. Li, Y. Yang, Highly efficient removal of adsorbed cationic dyes by dual-network chitosan-based hydrogel, Environ Res, 263 (2024) 120195. DOI: 10.1016/j.envres.2024.120195

[6] X. Wang, J. Jiang, W. Gao, Reviewing textile wastewater produced by industries: characteristics, environmental impacts, and treatment strategies, Water Sci Technol, 85 (2022) 2076-2096. DOI: 10.2166/wst.2022.088

[7] C.J. Ogugbue, T. Sawidis, Bioremediation and detoxification of synthetic wastewater containing triarylmethane dyes by aeromonas hydrophila isolated from industrial effluent, Biotechnol Res Int, 2011 (2011) 967925. DOI: 10.4061/2011/967925

[8] T. Robinson, G. McMullan, R. Marchant, P. Nigam, Remediation of dyes in textile effluent: a critical review on current treatment technologies with a proposed alternative, Bioresour Technol, 77 (2001) 247-255. DOI: 10.1016/s0960-8524(00)00080-8

[9] J. Lin, W. Ye, M. Xie, D.H. Seo, J. Luo, Y. Wan, B. Van der Bruggen, Environmental impacts and remediation of dye-containing wastewater, Nature Reviews Earth & Environment, 4 (2023) 785-803. DOI: 10.1038/s43017-023-00489-8

[10] S. Mondal, M.K. Purkait, S. De, Adsorption of Dyes, in: S. Mondal, M.K. Purkait, S. De (Eds.) Advances in Dye Removal Technologies, Springer Singapore, Singapore, 2018, pp. 49-98. DOI:10.1007/978-981-10-6293-3_2

[11] F. Taghizadeh, M. Ghaedi, K. Kamali, E. Sharifpour, R. Sahraie, M.K. Purkait, Comparison of nickel and/or zinc selenide nanoparticle loaded on activated carbon as efficient adsorbents for kinetic and equilibrium study of removal of Arsenazo (III) dye, Powder Technology, 245 (2013) 217-226. DOI: 10.1016/j.powtec.2013.04.020

[12] S. Bondock, A.A. El-Zahhar, M.M. Alghamdi, S. Keshk, Synthesis and evaluation of N-allylthiourea-modified chitosan for adsorptive removal of arsenazo III dye from aqueous solutions, Int J Biol Macromol, 137 (2019) 107-118. DOI: 10.1016/j.ijbiomac.2019.06.193
[13] S.A. Khan, D.R. Krishna, P. Shyamala, Determination of thermodynamic parameters for cloud point extraction of Arsenazo-III and Magdala Red dyes using mixed micelles: An essential requirement for high performance, Journal of the Indian Chemical Society, 98 (2021) 100142. DOI: 10.1016/j.jics.2021.100142
[14] S.B. Pillai, N.V. Thombre, Coagulation, flocculation, and precipitation in water and used water purification, in: Handbook of water and used water purification, Springer, 2024, pp. 3-27.
[15] V.K. Garg, R. Gupta, A. Bala Yadav, R. Kumar, Dye removal from aqueous solution by adsorption on treated sawdust, Bioresour Technol, 89 (2003) 121-124. DOI: 10.1016/s0960-8524(03)00058-0
[16] R. Olchowski, D.A. Giannakoudakis, I. Anastopoulos, M. Barczak, E. Zięba, R. Dobrowolski, J. Dobrzyńska, Arsenazo III removal from diagnostic laboratories wastewater by effective adsorption onto thermochemically modified ordered mesoporous carbon, Environmental Nanotechnology, Monitoring & Management, 16 (2021) 100607. DOI: 10.1016/j.enmm.2021.100607
[17] N.S. Awwad, A.Y. Alshahrani, E. El SayedMassoud, A. Bouzidi, M.S.A. Hussein, I.S. Yahia, Mechanism for microwave degradation of Methylene Blue and Arsenazo(III) dyes using graphene oxide synthesized from date pits, Desalination and Water Treatment, 187 (2020) 321-332. DOI: 10.5004/dwt.2020.25442
[18] S. Alharthi, M.O.A. El-Magied, Industrial by-product utilized synthesis of mesoporous aluminum silicate sorbent for thorium removal, Korean Journal of Chemical Engineering, 38 (2021) 2365-2374. DOI: 10.1007/s11814-021-0877-2
[19] S. Alharthi, S.A. Alharthy, E.S.A. Manaa, M.O. Abd El-Magied, W.M. Salem, High adsorption performance of Cr(VI) ions from the electroplating waste solution using surface-modified porous poly 2-((methacryloxy)methyl)oxirane polymers, Zeitschrift für anorganische und allgemeine Chemie, 648 (2022) e202100327. DOI: 10.1002/zaac.202100327
[20] S. Alharthi, H.A. Batakoushy, S.A. Alharthy, M.O. Abd El-Magied, W.M. Salem, Electro-analytical sensing of anti-hypotensive agents: application to dosage forms and human urine, Toxicol Res (Camb), 11 (2022) 245-254. DOI: 10.1093/toxres/tfac004
[21] M.M. Ibrahim, H.S. El-Sheshtawy, M.O. Abd El-Magied, E.-S.A. Manaa, M.A.M. Youssef, M.N. Kouraim, E.M. Eldesouky, A.S. Dhmees, A facile and cost-effective adsorbent derived from industrial iron-making slag for uranium removal, Journal of Radioanalytical and Nuclear Chemistry, 329 (2021) 1291-1300. DOI: 10.1007/s10967-021-07914-6
[22] M.M. Ibrahim, H.S. El-Sheshtawy, M.O. Abd El-Magied, A.S. Dhmees, Mesoporous Al2O3 derived from blast furnace slag as a cost-effective adsorbent for U (VI) removal from aqueous solutions, International Journal of Environmental Analytical Chemistry, 103 (2023) 2948-2964. DOI: 10.1080/03067319.2021.1900150
[23] I.M. Maafa, A.A.S. Alahl, M.O. Abd El-Magied, X. Cui, A.S. Dhmees, Eco-friendly self-terminated process for preparation of CaO catalyst based on chitosan production wastes for biodiesel production, Journal of Materials Research and Technology, 30 (2024) 1217-1227. DOI: 10.1016/j.jmrt.2024.03.091
[24] C. Hogendoorn, P. Roszczenko-Jasinska, N.C. Martinez-Gomez, J. de Graaff, P. Grassl, A. Pol, H.J.M. Op den Camp, L.J. Daumann, Facile Arsenazo III-Based Assay for Monitoring Rare Earth Element Depletion from Cultivation Media for Methanotrophic and Methylotrophic Bacteria, Appl Environ Microbiol, 84 (2018) e02887-02817. DOI: 10.1128/AEM.02887-17
[25] M.M. Rezk, A.S. Dhmees, M.O. Abd El-Magied, E.A. Manaa, H.S. El-Gendy, The influence of cobalt manganese ferrite nanoparticles (Co(0.5)Mn(0.5)Fe(2)O(4)) on reduction of hazardous effects of vanadate in adult rats, Toxicol Res (Camb), 9 (2020) 81-90. DOI: 10.1093/toxres/tfaa007
[26] M.O. Abd El-Magied, E.-S.A. Manaa, M.A.M. Youssef, M.N. Kouraim, A.S. Dhmees, E.M. Eldesouky, Uranium removal from aqueous medium using Co0.5Mn0.5Fe2O4 nanoparticles, Journal of Radioanalytical and Nuclear Chemistry, 327 (2021) 745-753. DOI: 10.1007/s10967-020-07571-1
[27] M.O. Abd El-Magied, M. Sopaih, Y.I. Bakr, M.M. Fawzy, Z.M. Anwar, M.M. Rezk, Design of some ferrite-based nanoparticles for uranium removal from Sella leach liquor, International Journal of Environmental Analytical Chemistry, (2024) 1-27. DOI: 10.1080/03067319.2024.2429009
[28] M.O. Abd El-Magied, Sorption of Uranium Ions from Their Aqueous Solution by Resins Containing Nanomagnetite Particles, Journal of Engineering, 2016 (2016) 1-11. DOI: 10.1155/2016/7214348
[29] M.O. Abd El-Magied, A.A. Tolba, H.S. El-Gendy, S.A. Zaki, A.A. Atia, Studies on the recovery of Th(IV) ions from nitric acid solutions using amino-magnetic glycidyl methacrylate resins and application to granite leach liquors, Hydrometallurgy, 169 (2017) 89-98. DOI: 10.1016/j.hydromet.2016.12.011
[30] A.M. Abu El-Soad, G. Lazzara, M.O. Abd El-Magied, G. Cavallaro, J.S. Al-Otaibi, M.I. Sayyed, E.G. Kovaleva, Chitosan Functionalized with Carboxyl Groups as a Recyclable Biomaterial for the Adsorption of Cu (II) and Zn (II) Ions in Aqueous Media, Int J Mol Sci, 23 (2022). DOI: 10.3390/ijms23042396
[31] A.M. Abu El-Soad, M.O. Abd El-Magied, N.A. Martemyanov, E.G. Kovaleva, Synthesis and characterization of amino-based carboxymethyl chitosan and its adsorption features towards Cu (II) and Zn (II) Ions, in: 5th International Conference" Modern Synthetic Methodologies for Creating Drugs and Functional Materials"(MOSM 2021): Book of Abstracts, Individual entrepreneur Shestakova Ekaterina Vyacheslavovna, Ekaterinburg, 2021, pp. PR-179.
[32] E. Rapo, S. Tonk, Factors Affecting Synthetic Dye Adsorption; Desorption Studies: A Review of Results from the Last Five Years (2017-2021), Molecules, 26 (2021) 5419. DOI: 10.3390/molecules26175419
[33] M.O. Abd El-Magied, High-efficiency recovery of cerium ions from monazite leach liquor by polyamines and polycarboxylates chitosan sorbents prepared from marine industrial wastes, Int J Biol Macromol, 243 (2023) 125243. DOI: 10.1016/j.ijbiomac.2023.125243

[34] E.A. Matter, A.S. Dhmees, W.M. Salem, M.O.A. El-Magied, G.H.G. Ahmed, Extraction of rare earth elements from monazite leach liquor using functionalized chitosan sorbents derived from shrimp waste, Environ Sci Pollut Res Int, 30 (2023) 108067-108084. DOI: 10.1007/s11356-023-29662-8
[35] J.S. Piccin, T.R.S.A. Cadaval, L.A.A. De Pinto, G.L. Dotto, Adsorption isotherms in liquid phase: experimental, modeling, and interpretations, Adsorption processes for water treatment and purification, (2017) 19-51. DOI: 10.1007/978-3-319-58136-1_2
[36] R.E. Kohler, Irving Langmuir and the" Octet" Theory of Valence, Historical studies in the physical sciences, 4 (1974) 39-87.
[37] H. Swenson, N.P. Stadie, Langmuir's Theory of Adsorption: A Centennial Review, Langmuir, 35 (2019) 5409-5426. DOI: 10.1021/acs.langmuir.9b00154
[38] A.M. Abu El-Soad, M.O. Abd El-Magied, M.S. Atrees, E.G. Kovaleva, G. Lazzara, Synthesis and characterization of modified sulfonated chitosan for beryllium recovery, Int J Biol Macromol, 139 (2019) 153-160. DOI: 10.1016/j.ijbiomac.2019.07.162
[39] L.A. Yousef, A.R. Bakry, M.O. Abd El-Magied, Uranium(VI) recovery from its leach liquor using zirconium molybdophosphate composite: kinetic, equilibrium and thermodynamic studies, Journal of Radioanalytical and Nuclear Chemistry, 323 (2019) 549-556. DOI: 10.1007/s10967-019-06871-5
[40] M.O. Abd El-Magied, M.M. Rezk, Y.I. Bakr, M.M. Fawzy, M. Sopaih, Z.M. Anwar, Removal of uranium ions from contaminated solutions by adsorption on cerium and lanthanum magnesium ferrite, Journal of Radioanalytical and Nuclear Chemistry, (2024) 1-18. DOI: 10.1007/s10967-024-09889-6
[41] X. Chen, M.F. Hossain, C. Duan, J. Lu, Y.F. Tsang, M.S. Islam, Y. Zhou, Isotherm models for adsorption of heavy metals from water - A review, Chemosphere, 307 (2022) 135545. DOI: 10.1016/j.chemosphere.2022.135545
[42] S.H. Negm, M.O. Abd El-Magied, W.M. El Maadawy, M.M. Abdel Aal, S.M. Abd El Dayem, M.A. Taher, K.A. Abd El-Rahem, M.N. Rashed, M.F. Cheira, Appreciatively Efficient Sorption Achievement to U(VI) from the El Sela Area by ZrO2/Chitosan, Separations, 9 (2022) 311. DOI: 10.3390/separations9100311
[43] G. Cerofolini, A unified theory for Freundlich, Dubinin-Radushkevich, and Temkin behaviors, Journal of Colloid and Interface Science, 86 (1982) 204-212. DOI: 10.1016/0021-9797(82)90058-3
[44] W.M. Semida, A.M. Hassan, T.F. Mohammaden, S.H. Negm, M.O.A. El-Magied, Microwave-Assisted Synthesis of Functionalized Chitosan Adsorbents for Cerium Adsorption from Aqueous Solutions, Radiochemistry, 65 (2023) 510-522. DOI: 10.1134/s1066362223040136
[45] A.M. Donia, A.A. Atia, E.M.M. Moussa, A.M. El-Sherif, M.O. Abd El-Magied, Removal of uranium(VI) from aqueous solutions using glycidyl methacrylate chelating resins, Hydrometallurgy, 95 (2009) 183-189. DOI: 10.1016/j.hydromet.2008.05.037